Spontaneous Symmetry Breaking in Bose-Einstein Condensates

Masahito UEDA

Tokyo Institute of Technology,
ERATO, JST

collaborators

Yuki Kawaguchi (Tokyo Institute of Technology)
Hiroki Saito (University of Electro-Communications)
Rina Kanamoto (University of Arizona)
Tatsuya Nakajima (Tohoku University)

	Superfluid helium	Atomic-gas BEC
Kinetics	**collision time** **collective mode** $\tau_{col} \sim 10^{-12}\text{s} << \omega^{-1}$ ⬇ • local equilibrium ensured • physics can be understood by conservation laws （energy, continuity eq. etc.） and hydrodynamics	$\tau_{col} \sim 10^{-3}\,\text{s} \sim \omega^{-1}$ ⬇ • not local equilibrium (Knudsen regime) • non-equilibrium relaxation and kinetics essential for BEC phase transition and vortex nucleation 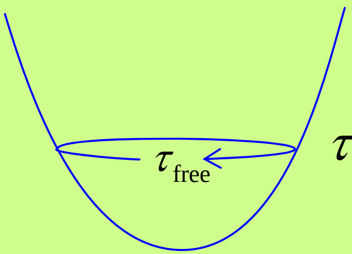 $\tau_{free} < \tau_{col}$
Magnetic moment Internal degrees of freedom	nuclear spin (^{3}He)	electronic spin ： BEC vs. magnetism • local control of spin texture • new phases such as cyclic phase
Symmetry breaking	• thermodynamic limit achieved • symmetry breaking of relative gauge ⬇ emergence of mean field	mesoscopic （not thermodynamic limit） ⬇ • symmetry breaking may or may not occur • dynamics of symmetry breaking should be observable

Outline of the talk

- **Scalar BEC**: soliton formation
  $\rightarrow$ breaking of translation symmetry

- **Rotating BEC**: vortex nucleation
  $\rightarrow$ breaking of axisymmetry

- **Spinor BEC**: spontaneous magnetization
  $\rightarrow$ breaking of rotational & chiral symmetries

- **Dipolar BEC**: spontaneous formation of spin textures
  $\rightarrow$ Einstein-de Haas effect
  ground-state mass flow

Symmetry breaking in a quasi-1D attractive BEC

R. Kanamoto, et al., PRA **67**, 013608 (2005)

- Mean-field description: the Gross-Pitaevskii equation

$$i\frac{\partial \psi_0}{\partial t}=\left(-\frac{\partial^2}{\partial \theta^2}+2\pi\gamma\left|\psi_0\right|^2\right)\psi_0,\quad \gamma\equiv\frac{UN}{2\pi}$$

dimensionless strength of interaction

$$\psi_0(\theta)=\psi_0(\theta+2\pi),\quad \int_0^{2\pi}\left|\psi_0\right|^2 d\theta=1$$

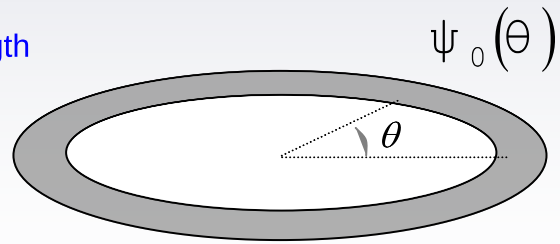

- Ground-state wave function

$|\gamma|\le 0.5$: The ground -state density is uniform.

$|\gamma|>0.5$: Translation symmmetry is spontaneously broken.

→ A bright soliton is formed.

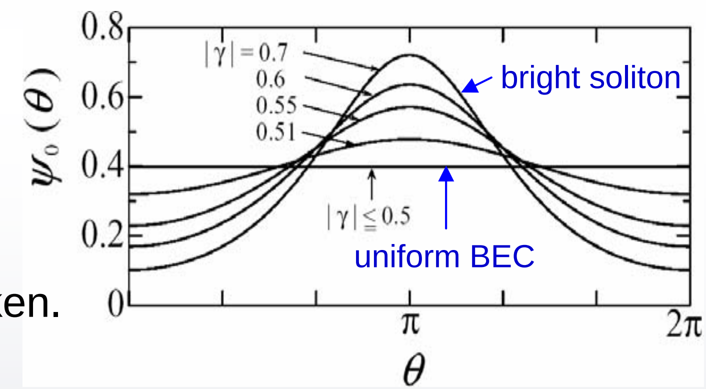

→ Mean field theory predicts a second-order quantum phase transition at γ = -1/2.

Bogoliubov spectrum before and after breaking the translational symmetry

uniform soliton

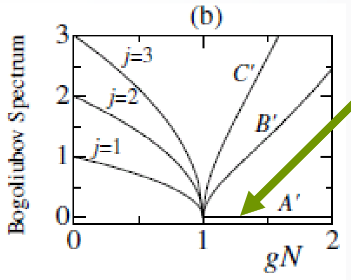

zero-energy mode: Goldstone mode associated with the breaking of translational symmetry

$gN=2|\gamma|$

FIG. 1. (a) Excitation spectrum obtained by exact diagonalization of Hamiltonian (1) for $N = 200$. The inset shows the corresponding result obtained with truncation $l_c = 2$ near the critical point. (b) Bogoliubov spectrum corresponding to (a), where branch A' represents the Goldstone mode, B' the breathing mode of a bright soliton, and C' the second harmonic of B'. (c) Energy gap ΔE between the ground and the first excited states in the many-body spectrum versus the total number of atoms N with $gN = 1.4$ held fixed. Triangles and circles denote results obtained with $l_c = 1$ and $l_c = 2$, respectively.

Many-body spectrum

R. Kanamoto, et al., PRL **94**, 090404(2005)

uniform BEC ↔ bright soliton

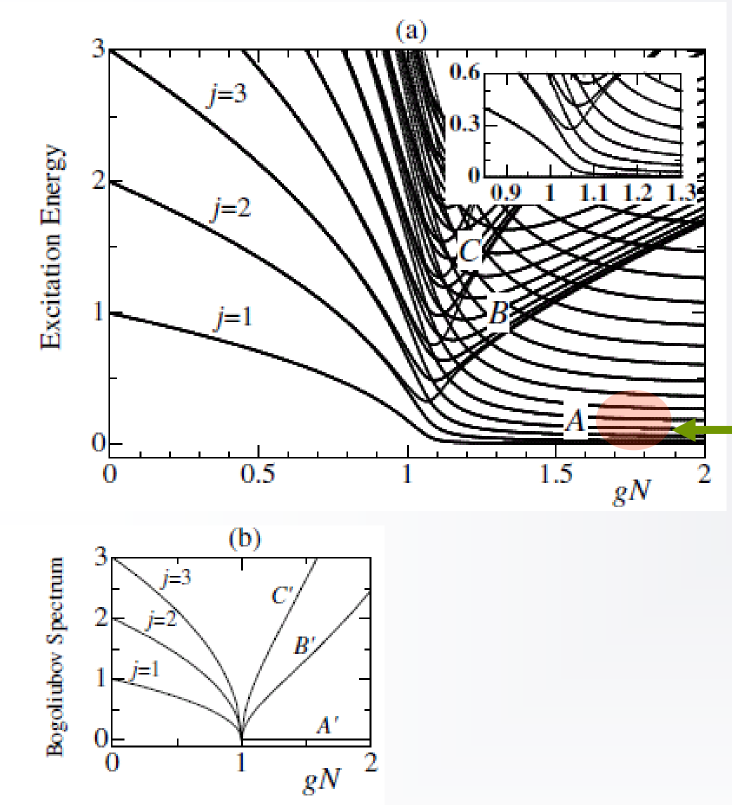

FIG. 1. (a) Excitation spectrum obtained by exact diagonalization of Hamiltonian (1) for $N = 200$. The inset shows the corresponding result obtained with truncation $l_c = 2$ near the critical point. (b) Bogoliubov spectrum corresponding to (a), where branch A' represents the Goldstone mode, B' the breathing mode of a bright soliton, and C' the second harmonic of B'. (c) Energy gap ΔE between the ground and the first excited states in the many-body spectrum versus the total number of atoms N with $gN = 1.4$ held fixed. Triangles and circles denote results obtained with $l_c = 1$ and $l_c = 2$, respectively.

The many-body spectrum in the uniform BEC is similar to that of the Bogoliubov spectrum. However, a dramatic change in the landscape of the energy spectrum occurs in the bright soliton regime.

In particular, a quasi-degenerate spectrum appears in the bright soliton regime.

This quasi-degeneracy is a signature of the symmetry breaking of translational symmetry that generates a bright soliton.

Many-body spectrum

R. Kanamoto, et al., PRL **94**, 090404(2005)

uniform BEC ↔ bright soliton

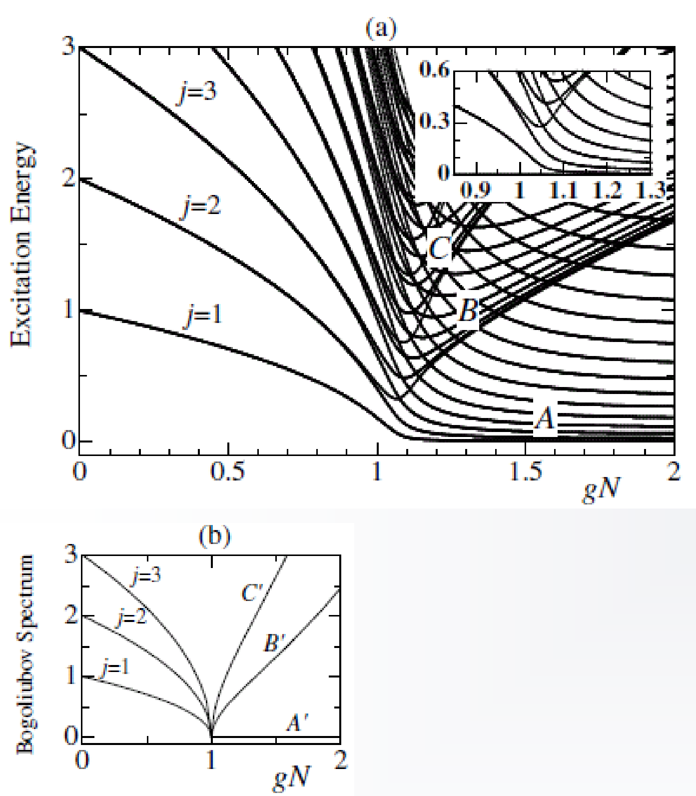

FIG. 1. (a) Excitation spectrum obtained by exact diagonalization of Hamiltonian (1) for $N = 200$. The inset shows the corresponding result obtained with truncation $l_c = 2$ near the critical point. (b) Bogoliubov spectrum corresponding to (a), where branch A' represents the Goldstone mode, B' the breathing mode of a bright soliton, and C' the second harmonic of B'. (c) Energy gap ΔE between the ground and the first excited states in the many-body spectrum versus the total number of atoms N with $gN = 1.4$ held fixed. Triangles and circles denote results obtained with $l_c = 1$ and $l_c = 2$, respectively.

It is remarkable that many-body physics can automatically generate such a symmetry breaking inducing quasi-degenerate spectrum which is absent at a mean-field level.

Rotating BEC

– symmetry breaking in vortex nucleation –

Vortex nucleation: ENS experiments

$\omega < \omega_c$

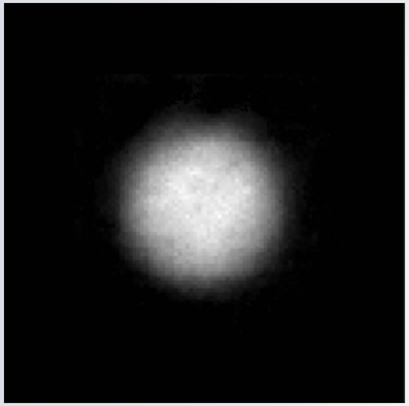

$\omega > \omega_c$

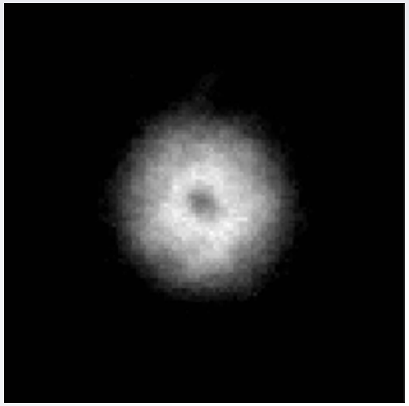

Between these two regimes there must be a nucleation process in which the axisymmetry of the system is spontaneously broken.

Such an axisymmetry breaking can be studied using mean-field theory.

Vortex nucleation: mean-field theory

D. Butts and D. Rokhsar, Nature **397**, 327 (1999)

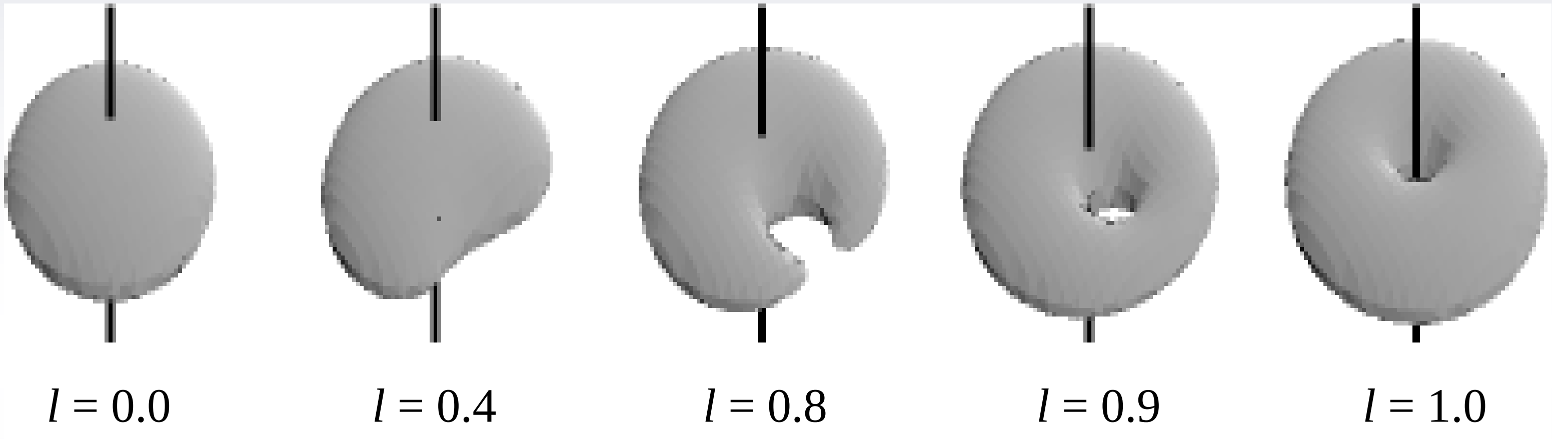

As the AM l increases, a vortex enters the system from the edge of the BEC by spontaneously breaking the axisymmetry of the system.

Does the many-body spectrum show quasi-degeneracy when the axisymmetry of the system is about to break?

Many-Body Excitation Spectrum of a Rotating BEC

T. Nakajima and MU, PRL **91,** 140401(2003)

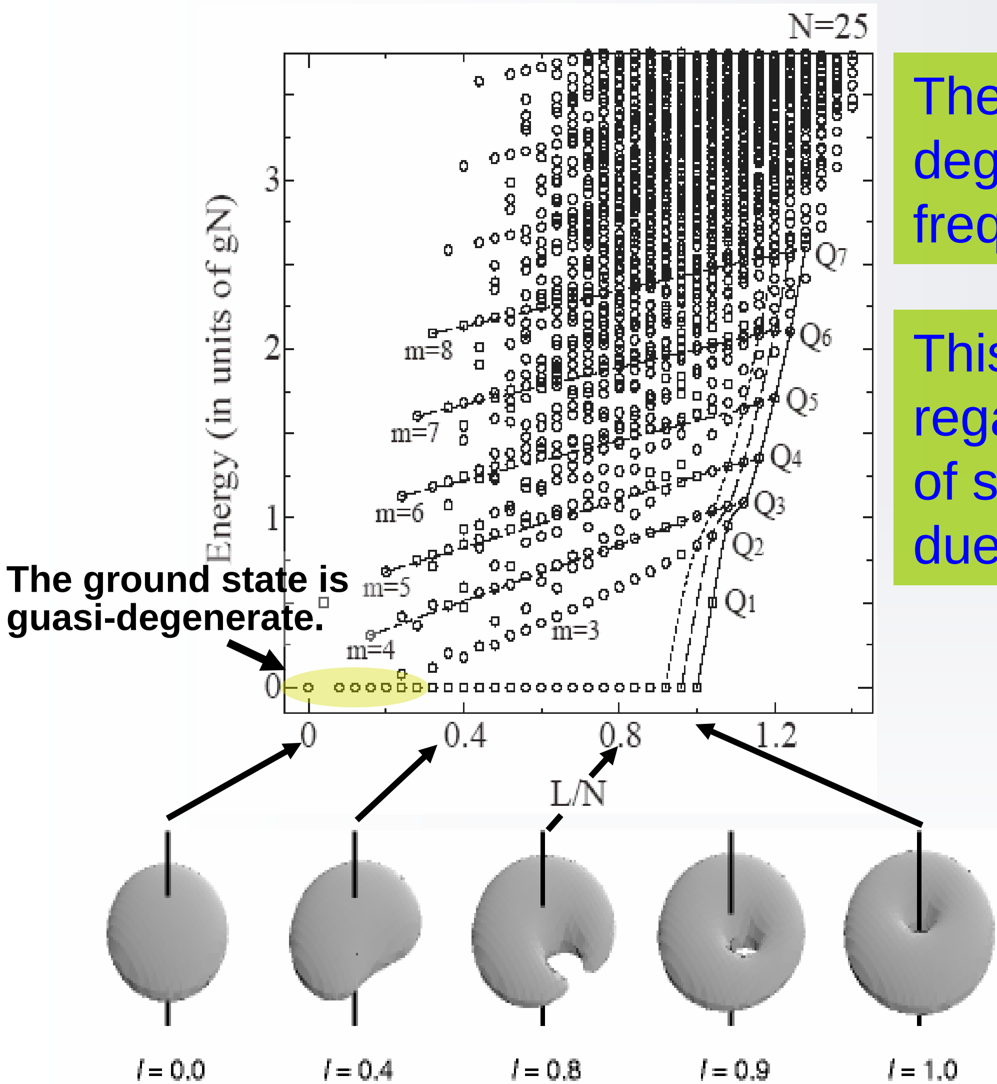

The ground state is quasi-degenerates when the rotational frequency is low.

This quasi-degeneracy may be regarded as a precursor of spontaneous symmetry breaking due to vortex nucleation.

Quasi-degenerate energy spectrum for N=256

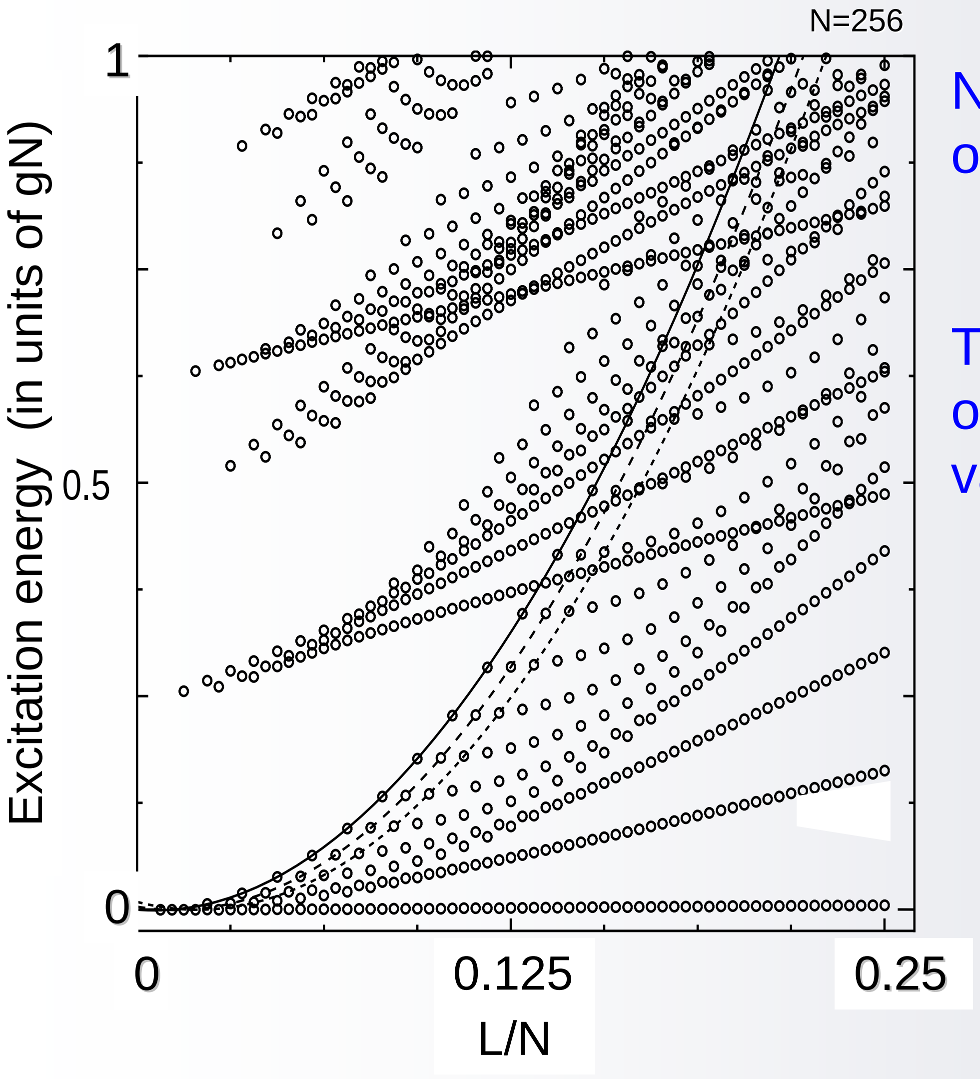

Note that the energy scale of this spectrum ~ *1/N*.

This quasi-degeneracy is solely of many-body nature and should vanish at the thermodynamic limit.

Quasi-degenerate energy spectrum for N=256

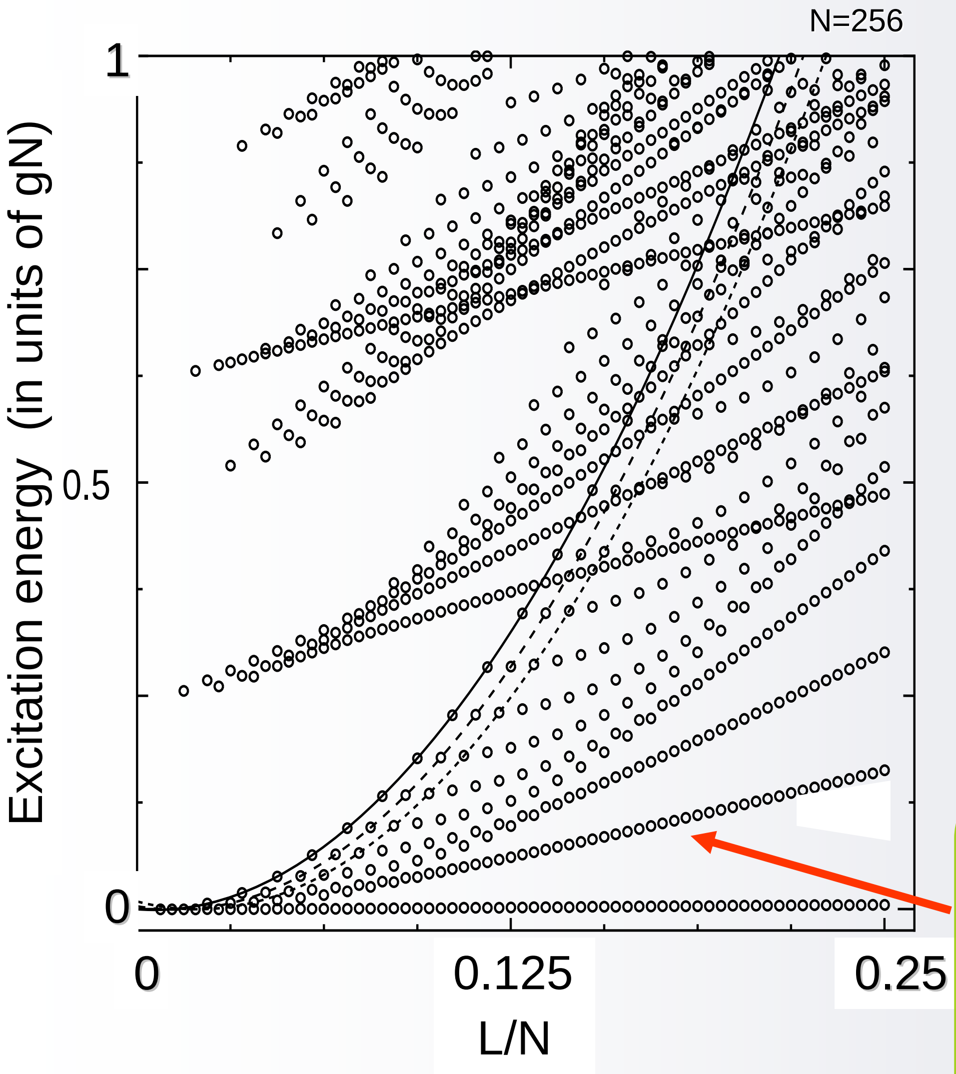

The Goldstone mode associated with the axisymmetry breaking is the lowest-lying envelope of the quasi-degenerete spectrum.

Universal Mechanism of Symmetry Breaking?

- It is striking that a many-body quasi-degenerate state is spontaneously generated when the continuous symmetry of the system is about to break and then removed when its role is over, i.e., after the symmetry has been broken.

- This mechanism for symmetry breaking appears universal, regardless of the details of the underlying physics, and manifests itself only in the mesoscopic regime.

- BEC systems offer an ideal testing ground for studying this problem.

Spinor BEC

– spontaneous formation of spin textures –

Spinor BEC

– Ferromagnetism vs. Spin Conservation –

How can the spontaneous magnetization of a ferromagnet occur in an isolated system in which the total angular momentum is conserved ?

One possible solution is that all spins align in the same direction because of the ferromagnetic interaction, but that the system is in a quantum-mechanical superposition state over all directions.

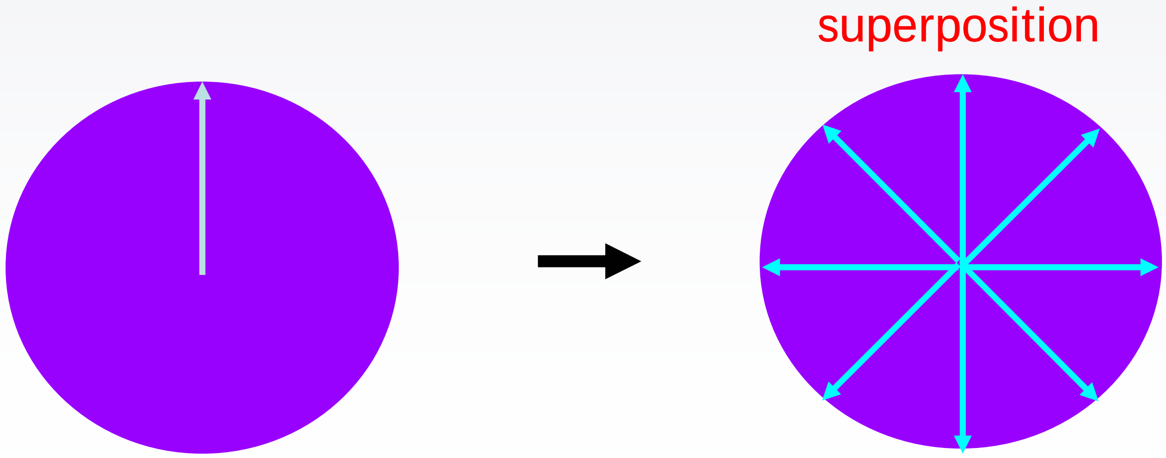

Spinor BEC

– Ferromagnetism vs. Spin Conservation –

How can the spontaneous magnetization of a ferromagnet occur in an isolated system in which the total angular momentum is conserved ?

The system develops local magnetic domains of various types that depend on

the nature of interaction,
conservation laws, and
the geometry of the trapping potential.

Spin-1 Ferromagnetic BEC in a Cigar-Shaped Trap

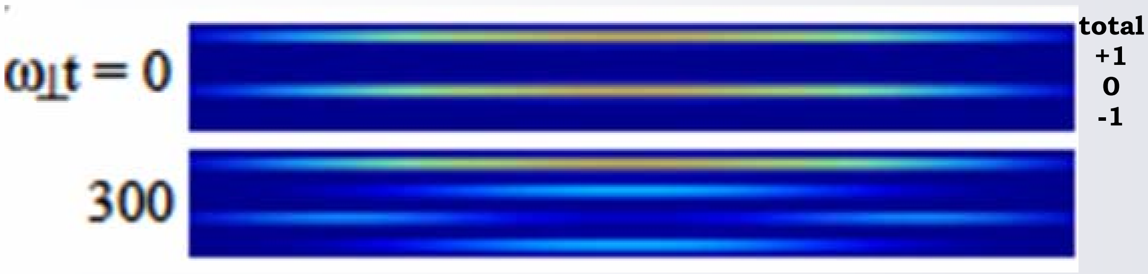

Initial state

$$\psi_1 = 0$$

$$\psi_0 = \sqrt{1-10^{-4}}\,\psi_g$$

$$\psi_1 = 0.01\psi_g$$

Observed
by Gakushuinn group!

$$(m=0)+(m=0)\leftrightarrow(m=1)+(m=-1)$$

spin-exhange
interaction

Spin-1 Ferromagnetic BEC in a Cigar-Shaped Trap

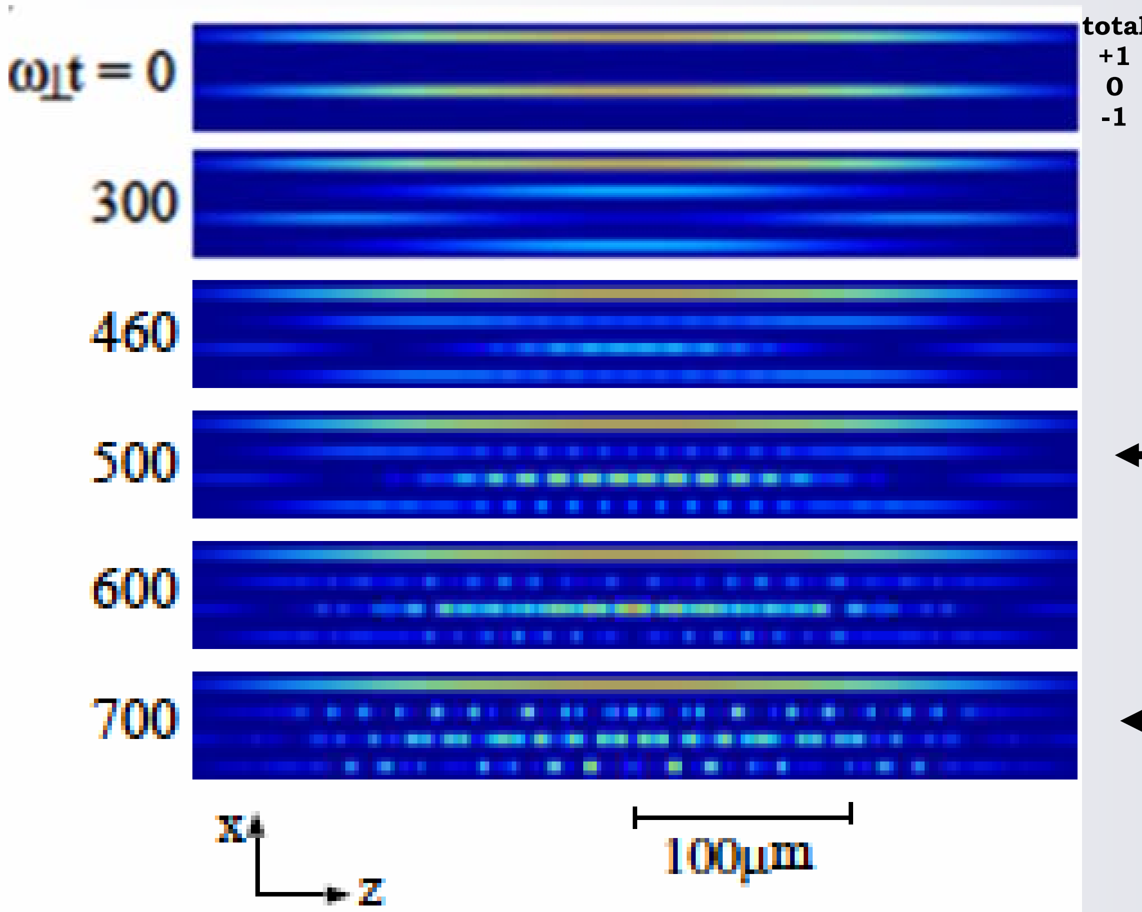

Initial state

$\psi_1 = 0$

$\psi_0 = \sqrt{1-10^{-4}}\,\psi_g$

$\psi_1 = 0.01\psi_g$

← dynamica instability

← Very irregular spin domains develop with each component almost equally populated.

H.Saito and M.Ueda, Phys. Rev. A**72**, 023610(2005)

Mean Spin Vector on the Trap Axis (r =0)

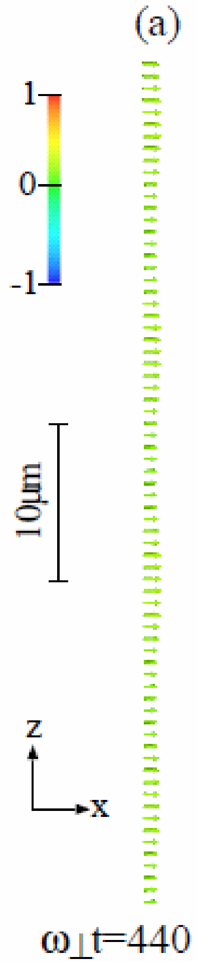

FIG. 3: The mean spin vectors $\boldsymbol{F}/n$ at $r = 0$ seen from the $-y$ direction, where the vertical axis is the z axis. The conditions are the same as those given in Fig. 1. The length of the spin vector is proportional to $|\boldsymbol{F}|/n$, and the color represents F_z/n according to the gauge shown at the top left corner. The spin vector is displayed from $z = 0$ to $z = 54\mu$m in (a)-(c), and from $z = 35\mu$m to $z = 89\mu$m in (d). The Larmor precession in the x-y plane is eliminated for clarity of presentation.

Because all particles are initially prepared in the *m=0* state, the length of the spin vector is zero everywhere.

Mean Spin Vector on the Trap Axis (r =0)

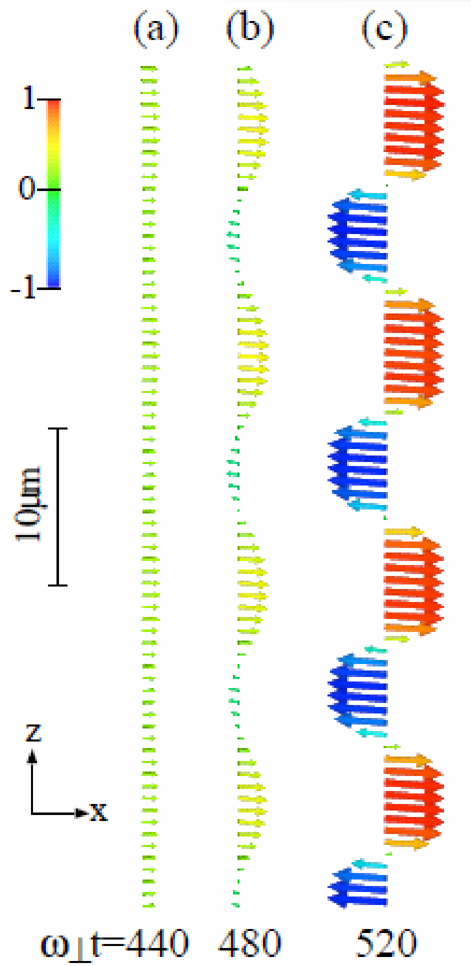

FIG. 3: The mean spin vectors $\boldsymbol{F}/n$ at $r = 0$ seen from the $-y$ direction, where the vertical axis is the z axis. The conditions are the same as those given in Fig. 1. The length of the spin vector is proportional to $|\boldsymbol{F}|/n$, and the color represents F_x/n according to the gauge shown at the top left corner. The spin vector is displayed from $z = 0$ to $z = 54\mu$m in (a)-(c), and from $z = 35\mu$m to $z = 89\mu$m in (d). The Larmor precession in the x-y plane is eliminated for clarity of presentation.

As time progresses, staggeed magnetic domains develop due to dynamical instability.

Mean Spin Vector on the Trap Axis (r =0)

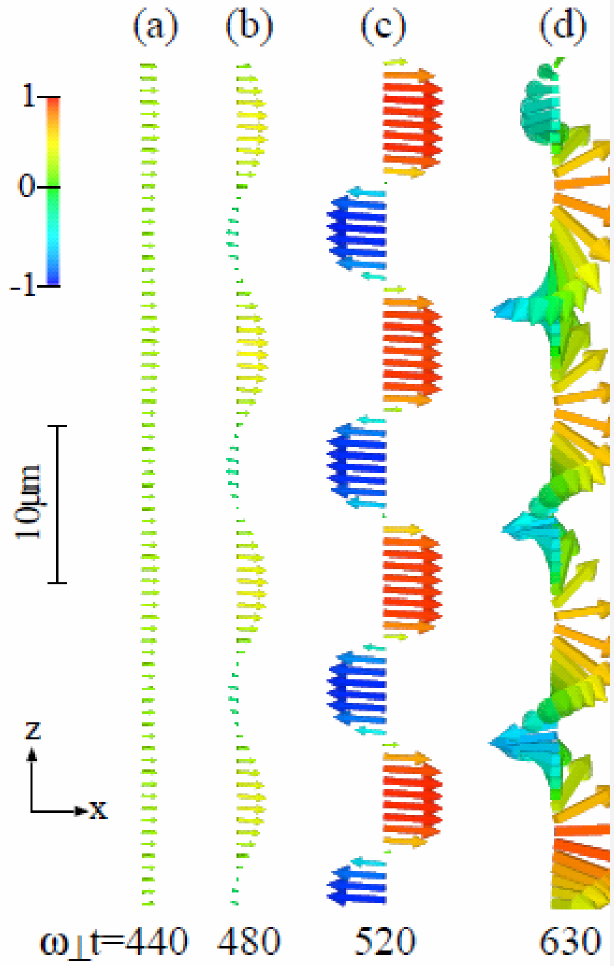

FIG. 3: The mean spin vectors $\boldsymbol{F}/n$ at $r=0$ seen from the $-y$ direction, where the vertical axis is the z axis. The conditions are the same as those given in Fig. 1. The length of the spin vector is proportional to $|\boldsymbol{F}|/n$, and the color represents F_x/n according to the gauge shown at the top left corner. The spin vector is displayed from $z=0$ to $z=54\mu$m in (a)-(c), and from $z=35\mu$m to $z=89\mu$m in (d). The Larmor precession in the x-y plane is eliminated for clarity of presentation.

After more time has elapsed, helical structures are spontaneously formed.

↓

Physical origin: competition between FM interaction and kinetic energy loss at the domain walls.

↓

Kinetic energy is decreased by the formation of a helix.

Spin Dynamics in a Pancake-Shaped Trap

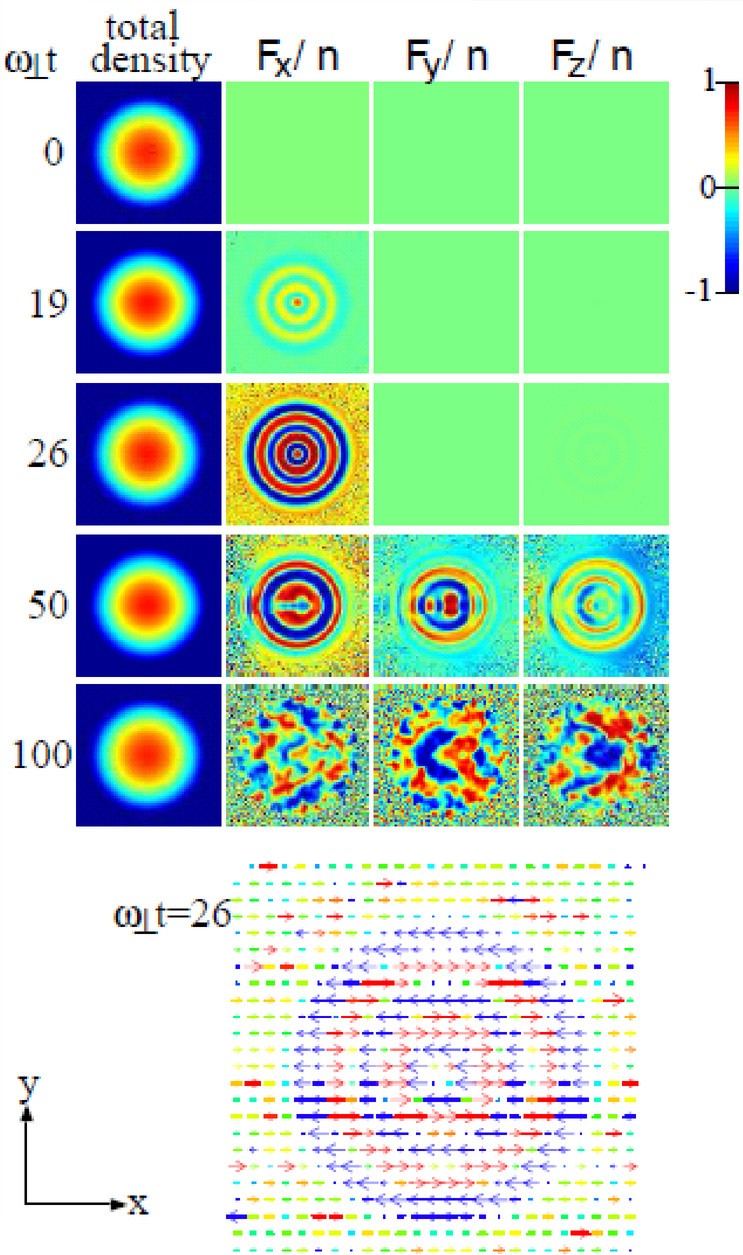

The concentric ring structure of the spin texture emerges due to dynamical instability.

Physical origin: the competition between the FM interaction and the kinetic energy under the constraints of spin conservation and the trap geometry.

1D: preferred spin texture is helix
2D: concentric rings

FIG. 4: The total density and the three components of the mean spin vector $\boldsymbol{F}/n$ of the two-dimensional system (from left to right panel), where the abscissa and ordinate refer to the x and y coordinates in real space. The size of each image is 48×48 in units of $(\hbar/m\omega_\perp)^{1/2}$. The color for the mean spin vector refers to the gauge. The bottom panel illustrates the direction of the spin at $\omega_\perp t = 26$, where the color represents F_z/n as shown in Fig. 3. The Larmor precession in the x-y plane is eliminated.

Ferromagnetic BEC

– chiral symmetry breaking –

Chiral Symmetry Breaking in a Ferromagnetic BEC

H.Saito, Y.Kawaguchi, and M.U., PRL **96**, 065302(2006)

Suppose that all atoms are prepared in the m=0 state in a pancake-shaped trap.

In the ⟷ region the modes with orbital angular momentum $l = \pm 1$ have imaginary parts; they are therefore dynamically unstable and grow exponentially.

Bogoliubov spectrum for l =0, ±1

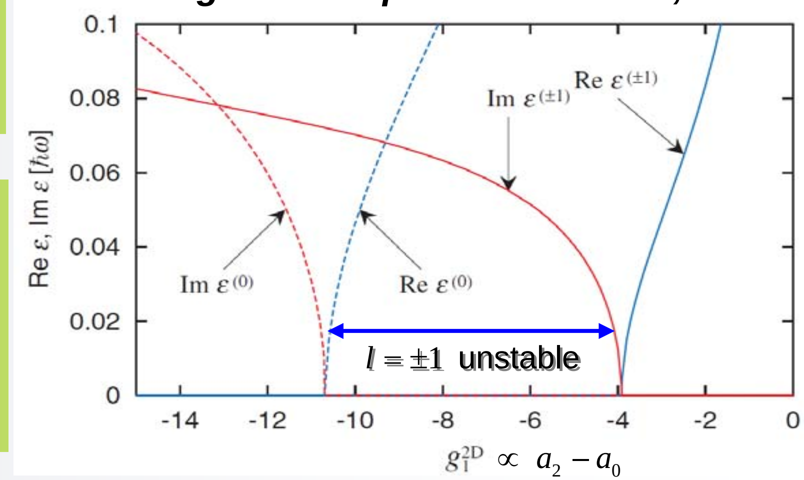

FIG. 1 (color). Real and imaginary parts of the lowest Bogoliubov energies $\varepsilon^{(\ell)}$ for $\ell = 0, \pm 1$, where the $m = \pm 1$ components of the eigenfunction are proportional to $e^{\pm i\ell\phi}$. The two energies $\varepsilon^{(\pm 1)}$ are degenerate due to the axisymmetry of the system. We have taken the parameters of spin-1 ^{87}Rb atoms, where the spin-independent interaction strength g_0^{2D} is related to the spin-dependent strength g_1^{2D} by $g_0^{2D} = -216.1 g_1^{2D}$.

Chiral Symmetry Breaking in a Ferromagnetic BEC

H.Saito, Y.Kawaguchi, and M.U., PRL **96**, 065302(2006)

Bogoliubov spectrum for l =0, ±1

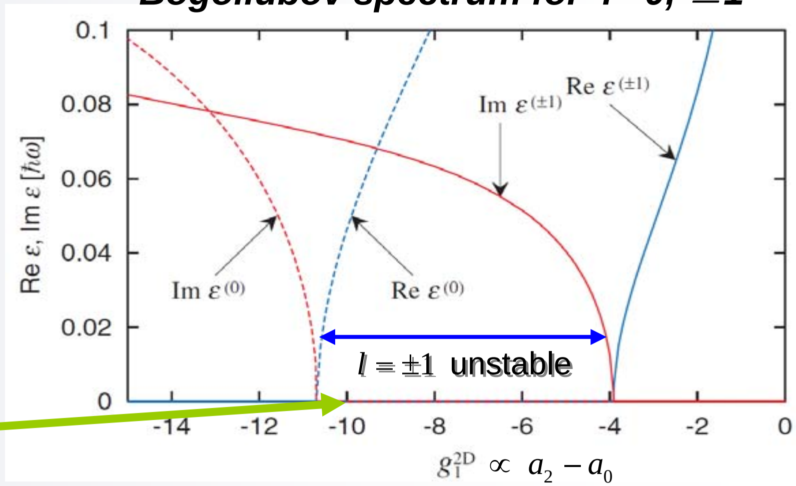

FIG. 1 (color). Real and imaginary parts of the lowest Bogoliubov energies $\varepsilon^{(\ell)}$ for $\ell = 0, \pm 1$, where the $m = \pm 1$ components of the eigenfunction are proportional to $e^{\pm i \ell \phi}$. The two energies $\varepsilon^{(\pm 1)}$ are degenerate due to the axisymmetry of the system. We have taken the parameters of spin-1 ^{87}Rb atoms, where the spin-independent interaction strength g_0^{2D} is related to the spin-dependent strength g_1^{2D} by $g_0^{2D} = -216.1 g_1^{2D}$.

Suppose that the parameter of ^{87}Rb BEC is prepared at

Then the system has orbital AM instability.

Prediction: the $l = \pm 1$ modes will start growing and rotate spontaneously!

Chiral Symmetry Breaking in a Ferromagnetic BEC

The angular momentum conservation implies that the *l =1* and *l = -1* modes must be created simultaneously by the same amount.

There are two possibilities:

spin	orbital		spin	orbital
$m=1$	$l=1$	degenerate	$m=1$	$l=-1$
$m=-1$	$l=-1$	$\longleftrightarrow$	$m=-1$	$l=1$

These two possibilities are degenerate, this degeneracy being a statement of the chiral symmetry.

Chiral Symmetry Breaking in a Ferromagnetic BEC

The chirally symmetric state has higher energy than the chiral-symmetry broken states.

Therefore the chiral symmetry is dynamically broken and each spin component begin to rotate spontaneously.

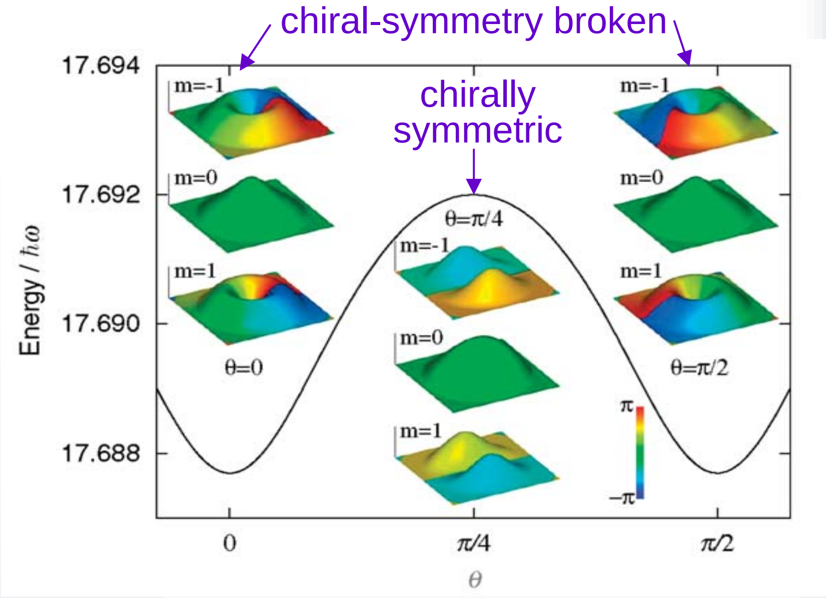

Time development of orbital AM l =-1 component

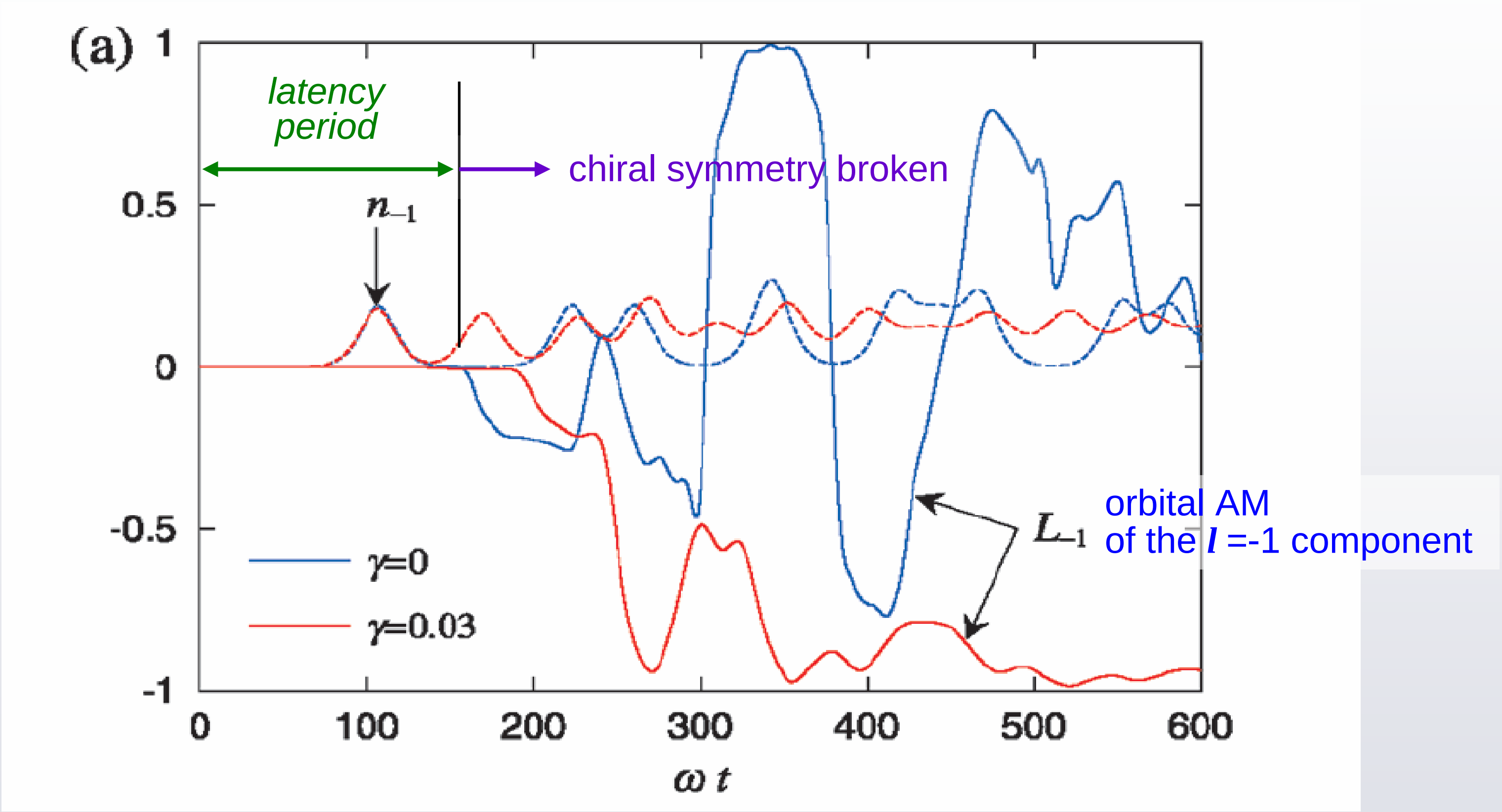

Spin Textures for Chirally Symmetric and Broken States

symmetric　　broken　　with dissipation

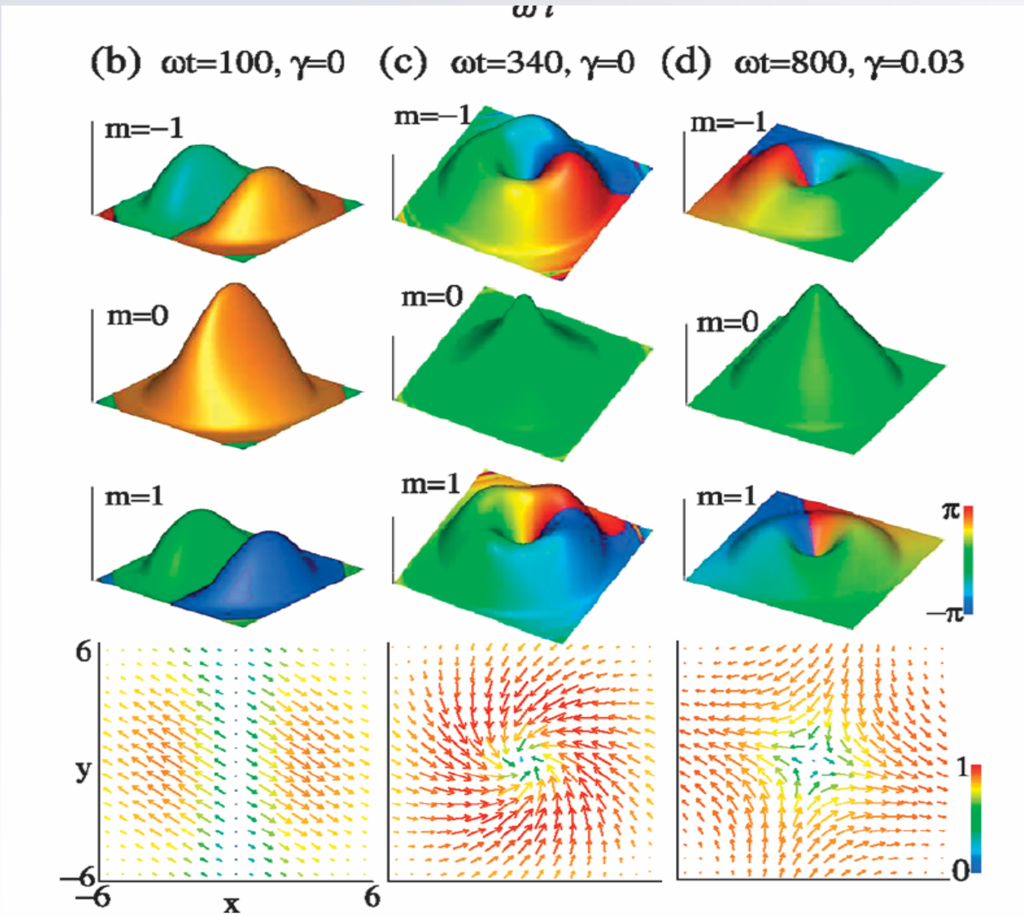

domain wall　　topological spin textures

The chirally symmetric state has a domain wall at the cost of the ferromagnetic interaction energy.

The chiral-symmetry-broken state circumvents this energy cost by developing topological spin textures.

→underlying physics of the chiral symmetry breaking

Prediction observed by the Berkeley group!

L. E. Sadler, et al., cond-mat/0605351

unmagnetized for a latency period

spontaneous magnetization

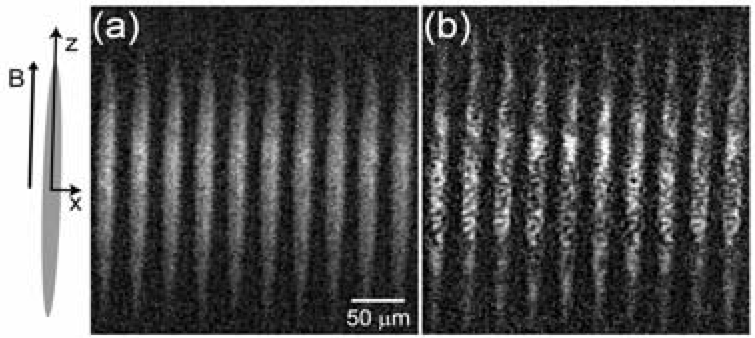

FIG. 1: Direct imaging of inhomogeneous spontaneous magnetization of a spinor BEC. Transverse imaging sequences (first 10 of 24 frames taken) are shown (a) for a single condensate probed at $T_{\text{hold}} = 36$ ms and (b) for a different condensate at $T_{\text{hold}} = 216$ ms. Shortly after the quench, the system remains in the unmagnetized $|m_z = 0\rangle$ state, showing neither short-range spatial nor temporal variation (i.e. between frames). In contrast, condensates at longer times are spatially inhomogeneous and display spontaneous Larmor precession as indicated by the cyclical variation of signal strength vs. frame number. Orientations of axes and of the magnetic field are shown at left.

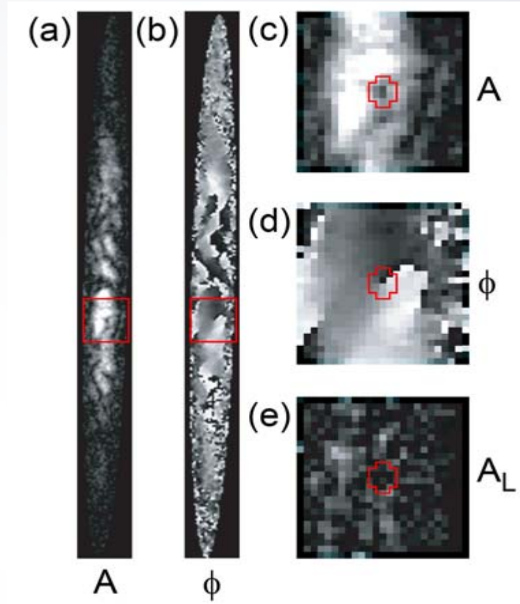

polar core spin-vortex

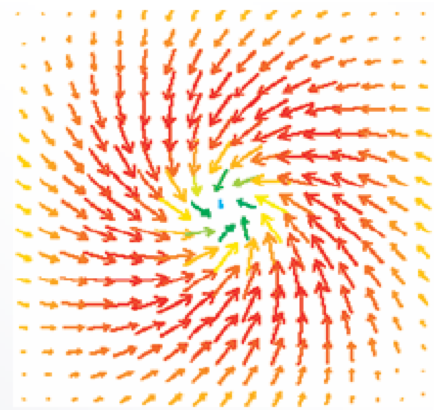

chiral-symmetry broken states

Dipolar BEC

– Einstein-de Haas effect –

– Ground-state circulation –

Magnetic Dipole-Dipole Interaction: Tensor Force

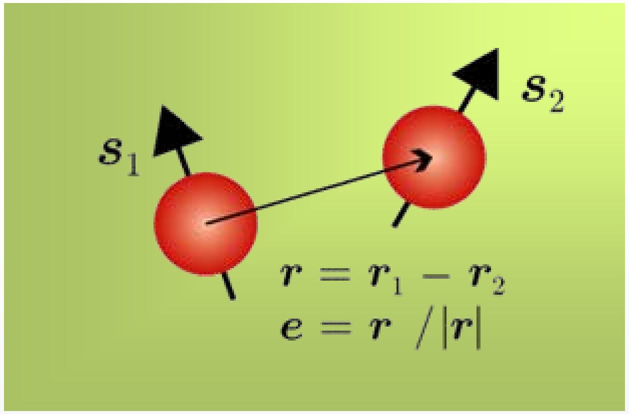

magnetic dipole moment $\boldsymbol{\mu} \sim g\mu_{\mathrm{B}}\boldsymbol{s}$

$$V_{\mathrm{dd}} = c_{\mathrm{dd}} \frac{(\boldsymbol{s}_1 \cdot \boldsymbol{s}_2) - 3(\boldsymbol{s}_1 \cdot \boldsymbol{e})(\boldsymbol{s}_2 \cdot \boldsymbol{e})}{|\boldsymbol{r}|^3}$$

$$c_{\mathrm{dd}} = \frac{\mu_0}{4\pi}(g\mu_{\mathrm{B}})^2$$

- Spin-orbit coupling
  - long-ranged
  - anisotropic

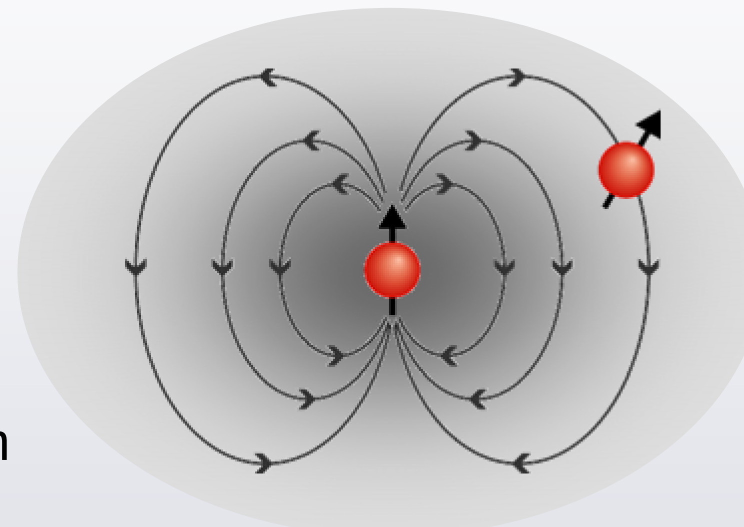

- Conserved quantity :
  total (spin+orbital) angular momentum

- Spin-exchange dynamics transfer angular momentum between spin and orbit, thereby spontaneously generating spin textures in an inhomogeneous trapped system.

Einstein-de Haas Effect in a Cr BEC

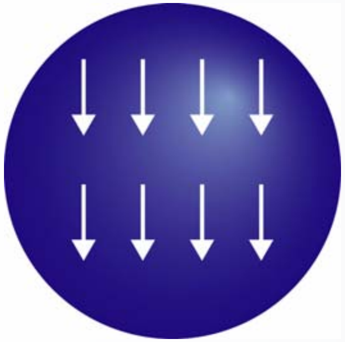

- Spin-polarized ^{52}Cr BEC created under a relatively strong magnetic field

Griesmaier et al., PRL **94**, 160401 (2005)

- What would happen to this BEC if $B \rightarrow 0$?

- Spin relaxation due to the dipole interaction
$\rightarrow$ Because of the conservation of the total AM, BEC would start to rotate spontaneously.

$\downarrow$

Einstein-de Haas effect

Einstein-de Haas Effect in a Cr BEC

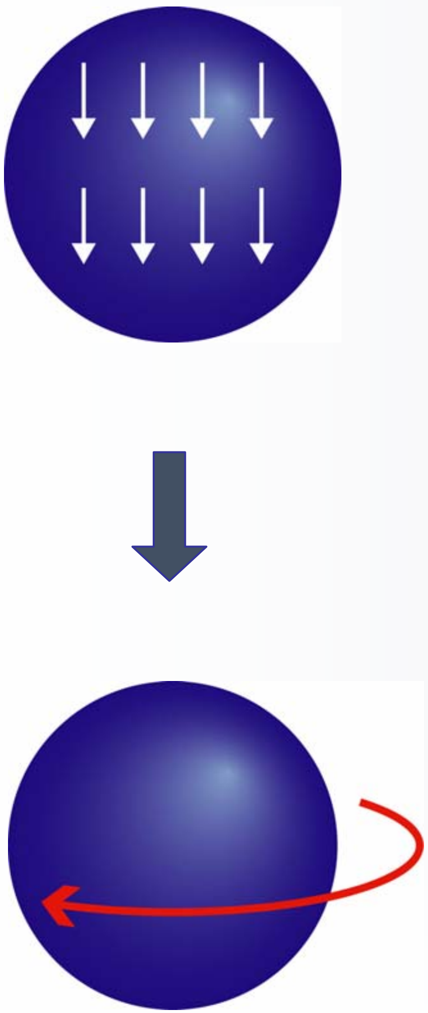

- 7 components non-local GP equation in 3D
- BEC begins to rotate spontaneously to compensate for a decrease in the spin angular momentum.

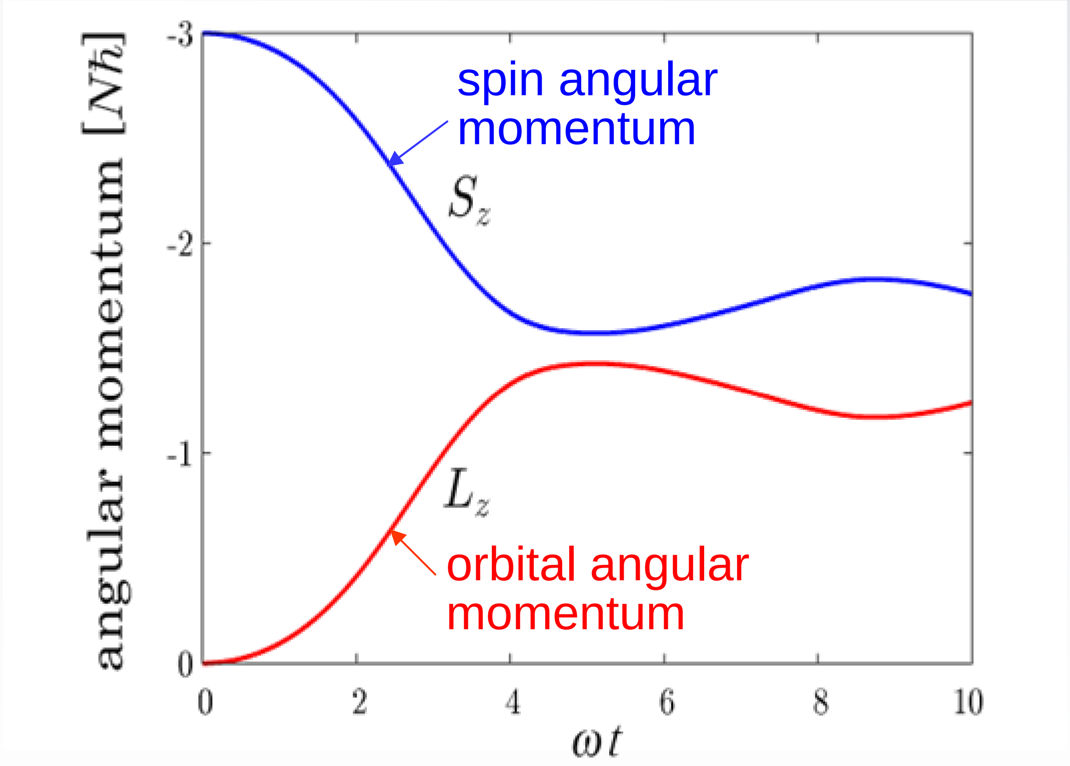

K. Kawaguchi, et al., PRL **96**, 080405(2006)
see also L. Santos and T. Pfau, PRL **96**, 190404(2006)

Einstein-de Haas Effect in a Cr BEC

K. Kawaguchi, et al., PRL **96**, 080405(2006)

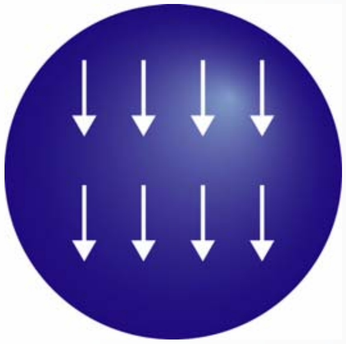

Atomic spins undergo Larmor precession around the local dipole field, and develop topological spin textures.

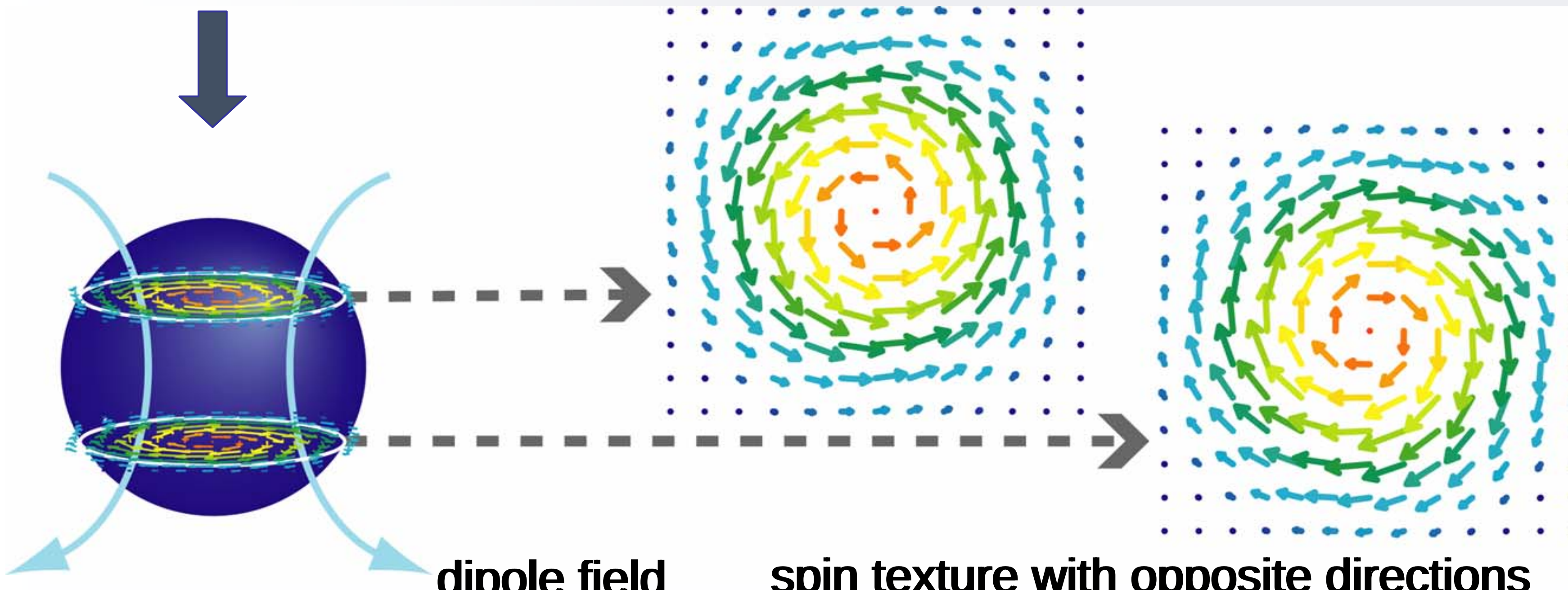

Spontaneous Circulation in the Ground State

- The magnetic dipole-dipole interaction in a solid-state ferromagnet is known to yield a rich variety of spin (domain) structures.
- The Einstein-de Haas effect is also known to occur in a ferromagnet.

What, then, is truly new in spinor-dipolar BECs?

Spontaneous Circulation in the Ground State

- The unique feature of the spinor-dipolar BEC that is absent from a solid-state ferromagnet is the spin-gauge symmetry which can transform
  spin texture $\longrightarrow$ mass current.

- The fundamental query is whether or not a spinor-dipolar BEC can exhibit a ***spontaneous net mass current*** in the ground state.

Ground-State Phase Diagram of Spin-1 Ferromagnetic BEC

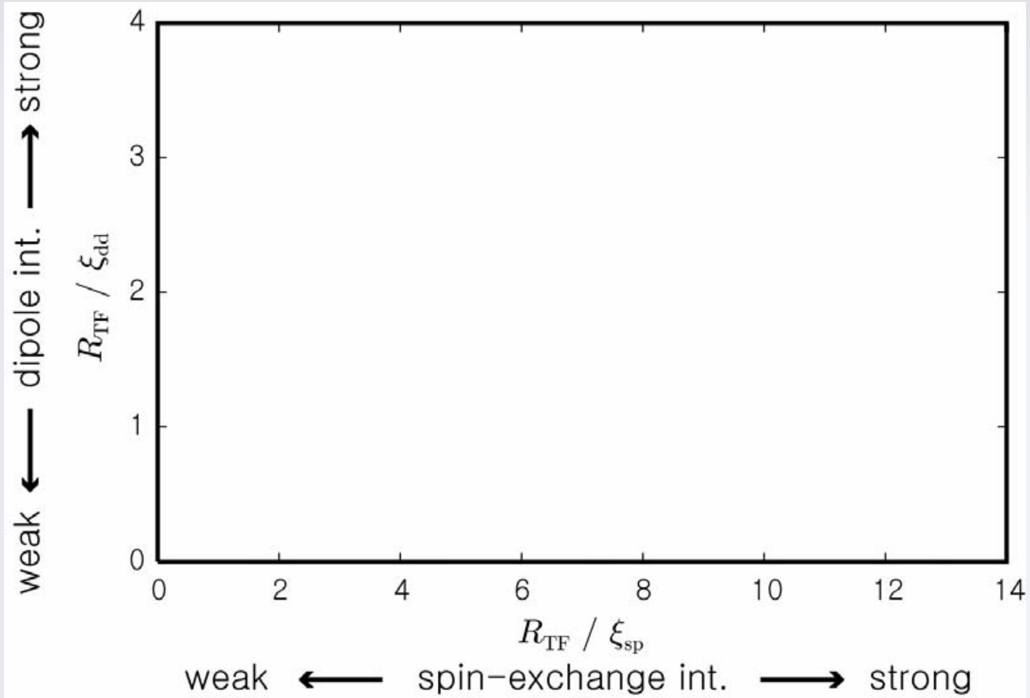

$$\xi_{\mathrm{dd}} = \hbar / \sqrt{2M\, c_{\mathrm{dd}} n_0}$$

$$\xi_{\mathrm{sp}} = \hbar / \sqrt{2M\, |g_1| n_0}$$

$$R_{\mathrm{TF}} = 2a_{\mathrm{ho}} \sqrt{g_0 n_0 / \hbar\omega}$$

$$U_{\mathrm{trap}}(\boldsymbol{r}) = \frac{1}{2} M\omega (x^2 + y^2 + z^2)$$

n_0 : TF peak density

$a_{\mathrm{ho}} = \sqrt{\hbar / M\omega}$

We have found three phases.

Phase Diagram Ⅰ: Flower Phase

to appear in PRL, cond-mat/ 0606288

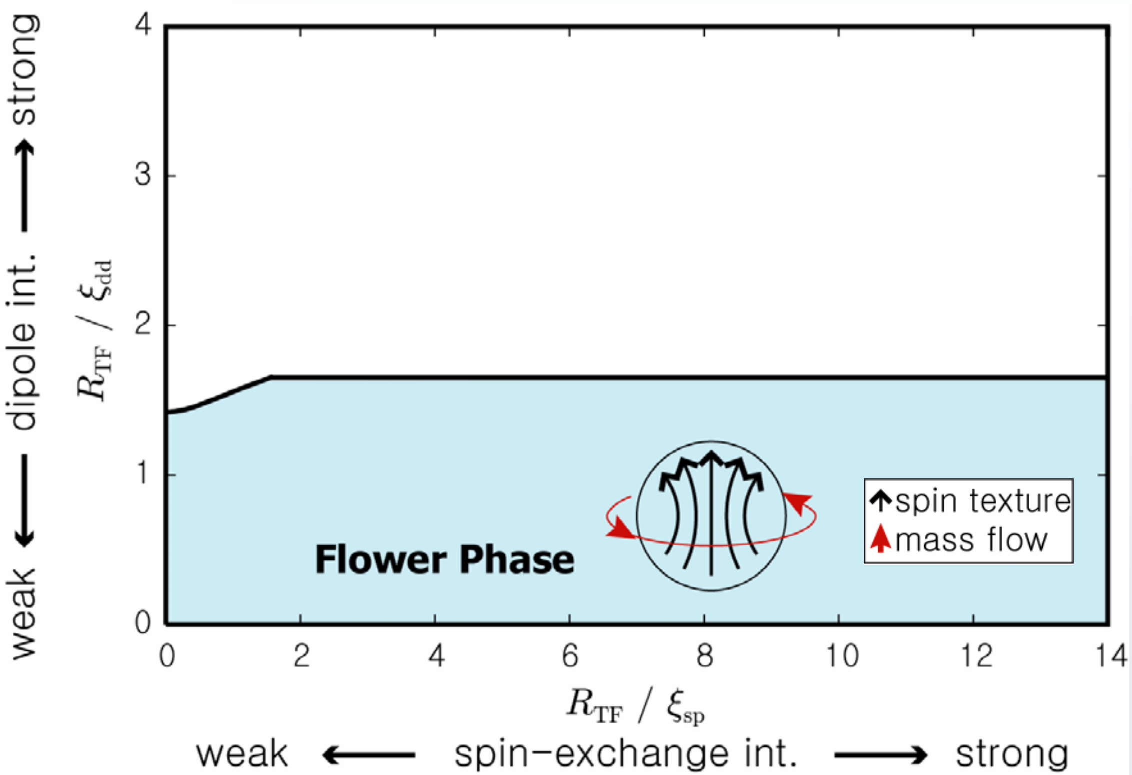

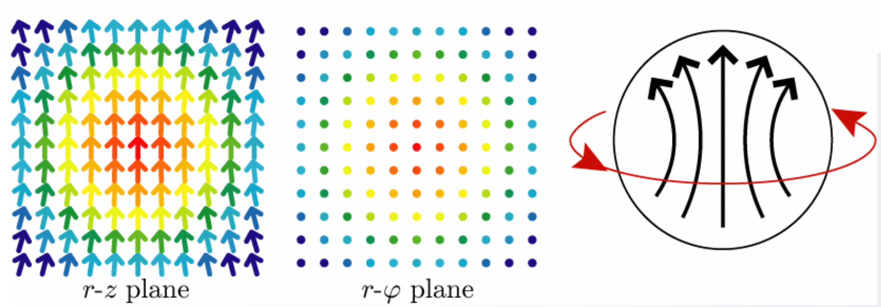

- spins almost polarized
- slightly bent outwards due to the dipole int.

Phase Diagram Ⅰ: Flower Phase

to appear in PRL, cond-mat/ 0606288

spin m_F	orbital winding	
1	0	← most atoms
0	1	
–1	2	

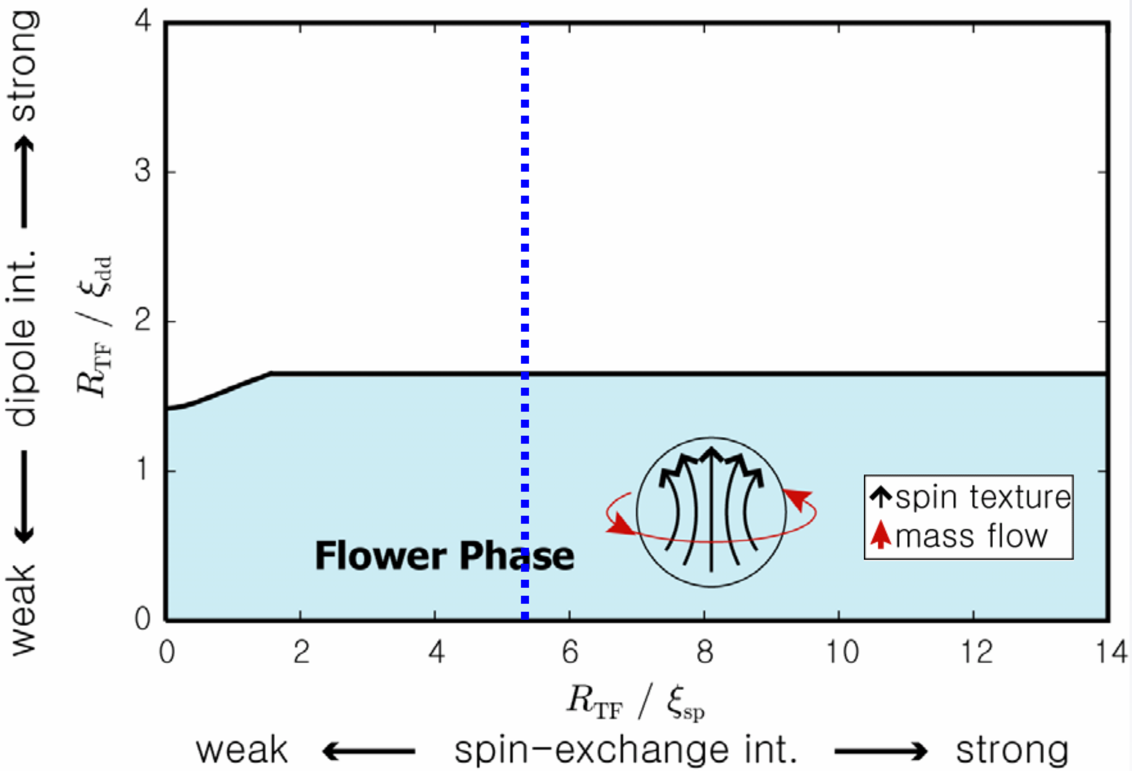

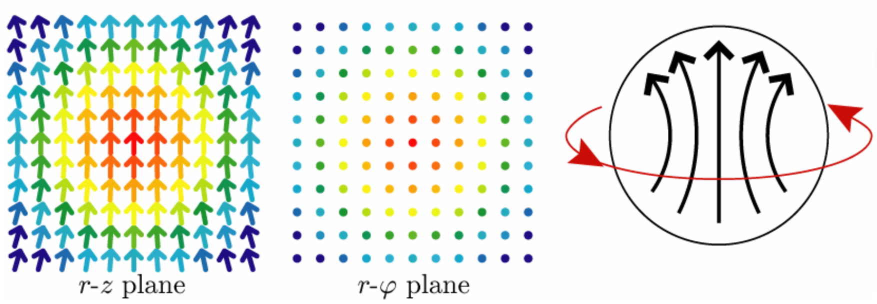

- most atoms in m_F=1 state
- orbital AM very small
- Each atom has unit total AM carried mostly by spin.

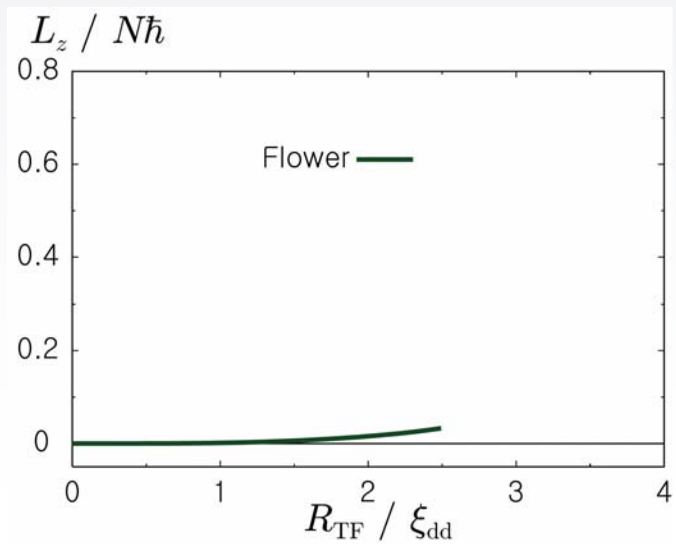

Phase Diagram Ⅱ : Chiral Spin-Vortex Phase

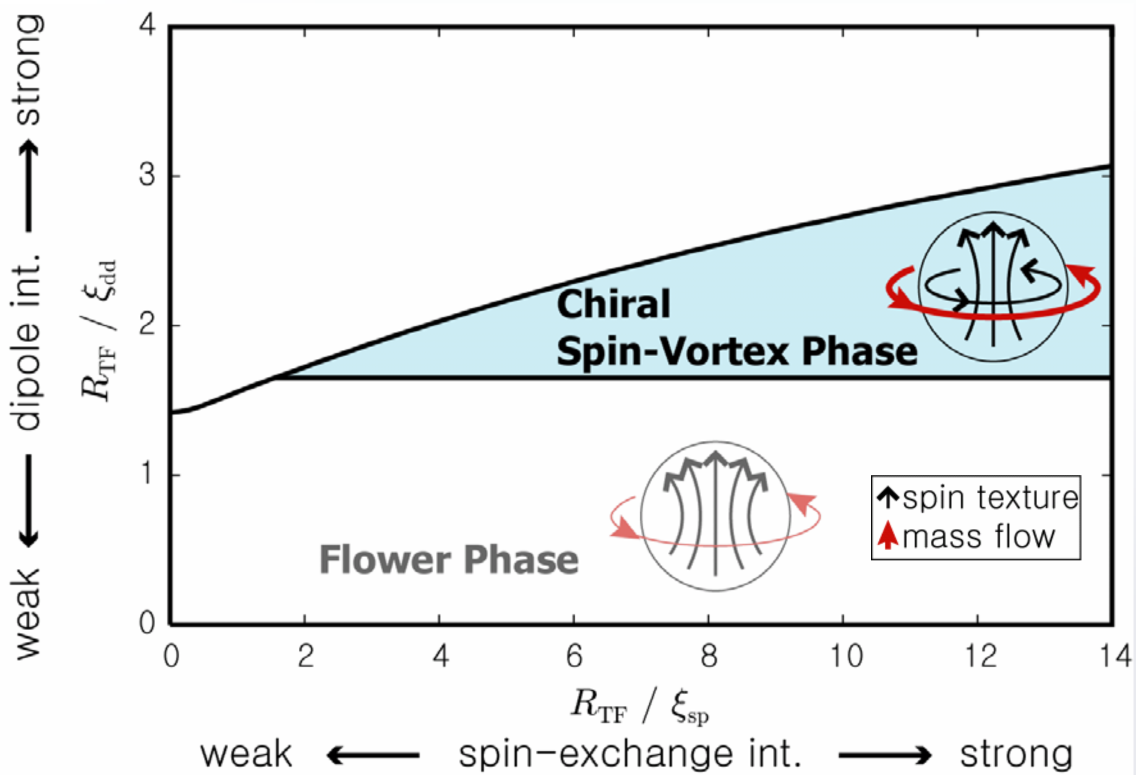

m_F	winding
1	0
0	1
–1	2

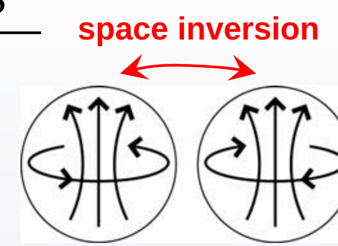

- dipole int. stronger
  →Spin circulates around the symmetry axis.
- clockwise and anti-clockwise spin circulations degenerate

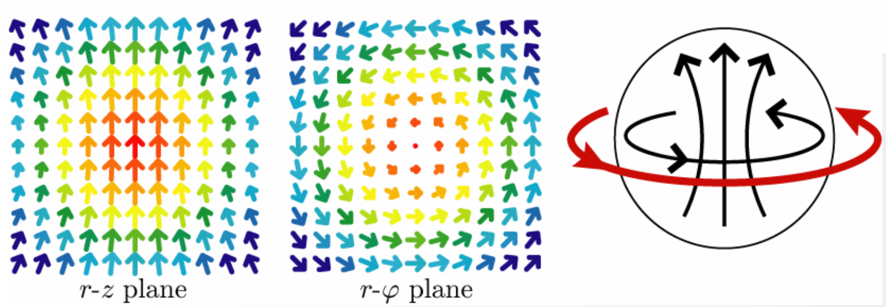

Phase Diagram Ⅱ: Chiral Spin-Vortex Phase

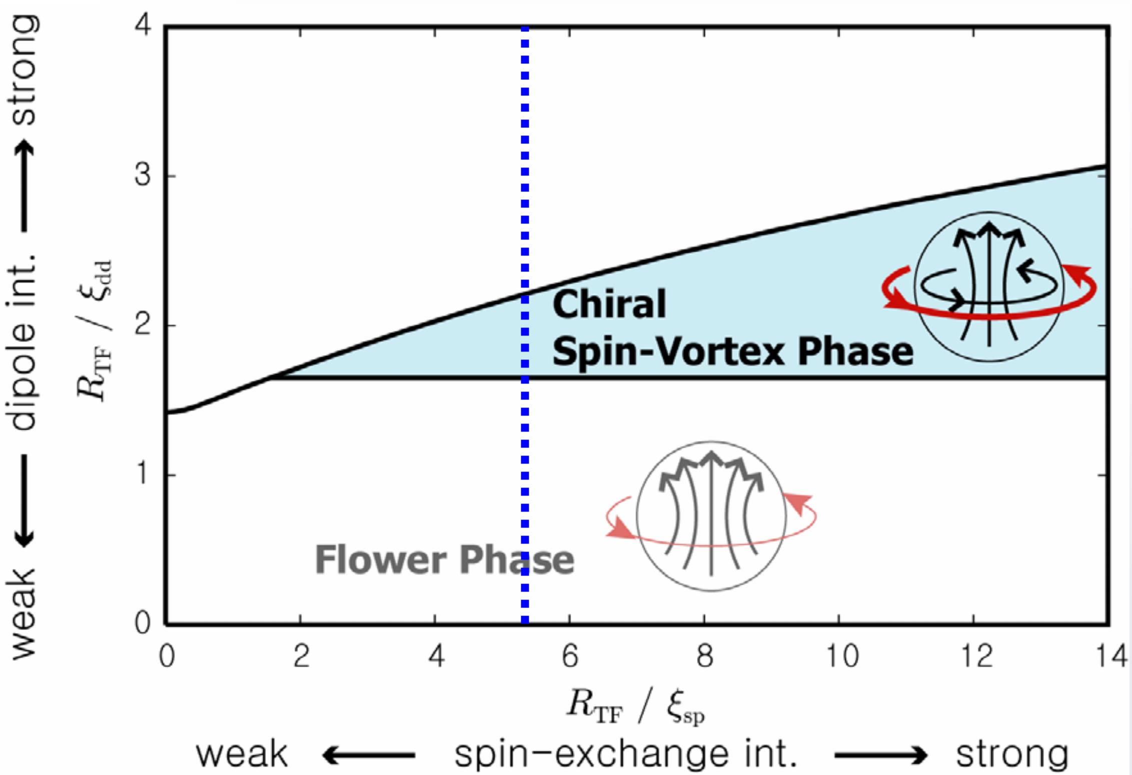

m_F	winding
1	0
0	1
–1	2

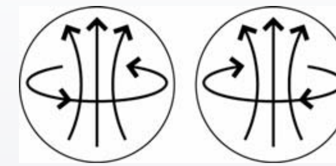

- chiral symmetry is broken

➔ substantial orbital AM hence a net mass current in the GS

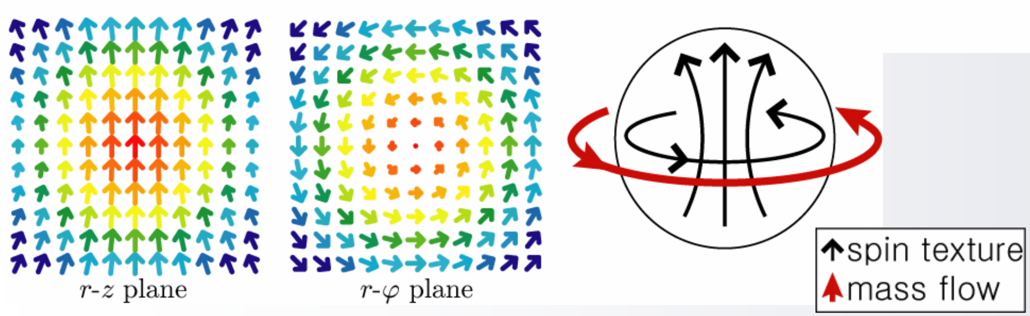

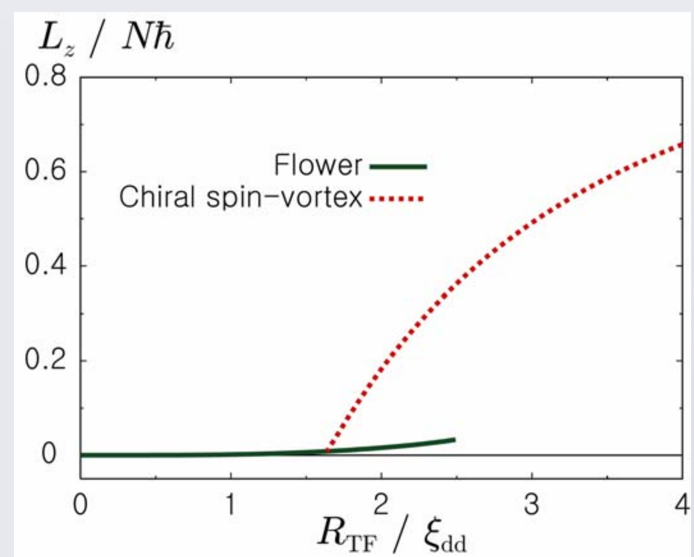

Phase Diagram Ⅲ: Polar-Core Vortex Phase

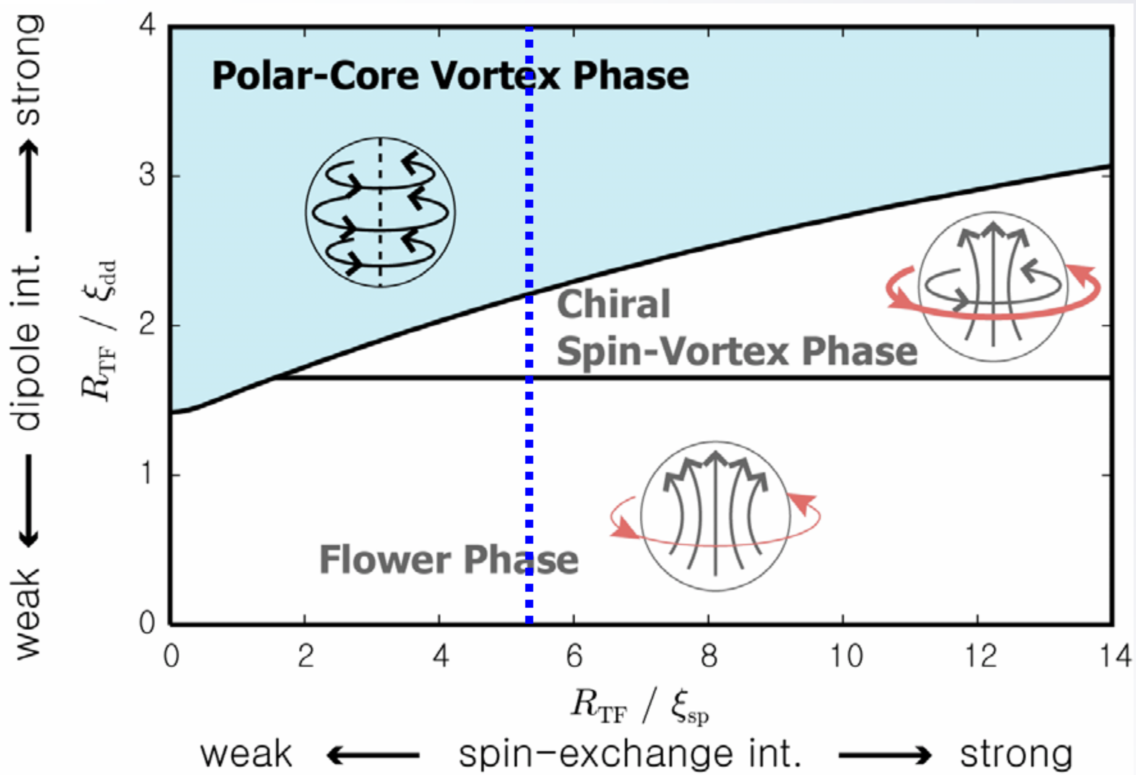

m_F	winding
1	-1
0	0
–1	1

- $N_1 = N_{-1}$: total spin 0
- total orbital AM 0
- S=0 & n≠0 at the core

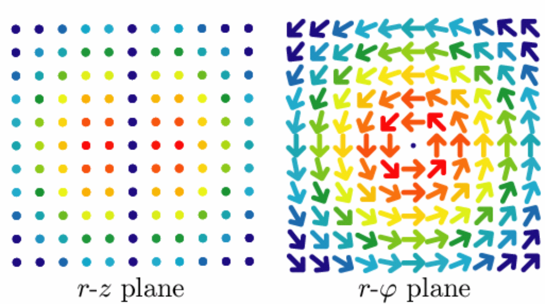

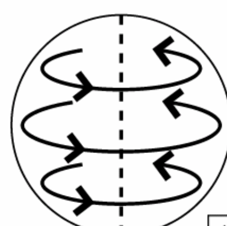

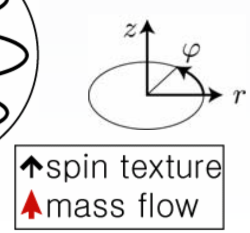

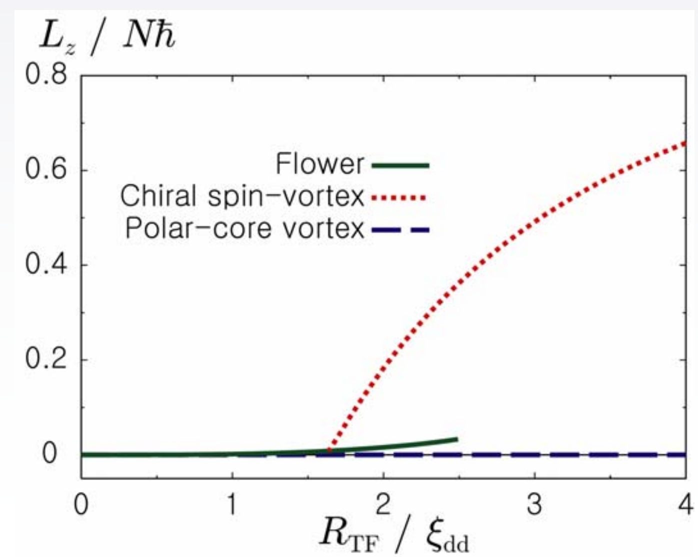

Time Reversal and Space Inversion Symmetries

Phase	J	P	T	PT
PCV	0	×	×	○
FL	1	○	×	×
CSV	1	×	×	×

FIG. 2: Broken (×) and unbroken (○) symmetries for each phase in Fig. 1. The schematic in each cell shows the spin configuration after the transformation by P, T, and PT.

Spin-1 ^{87}Rb BEC

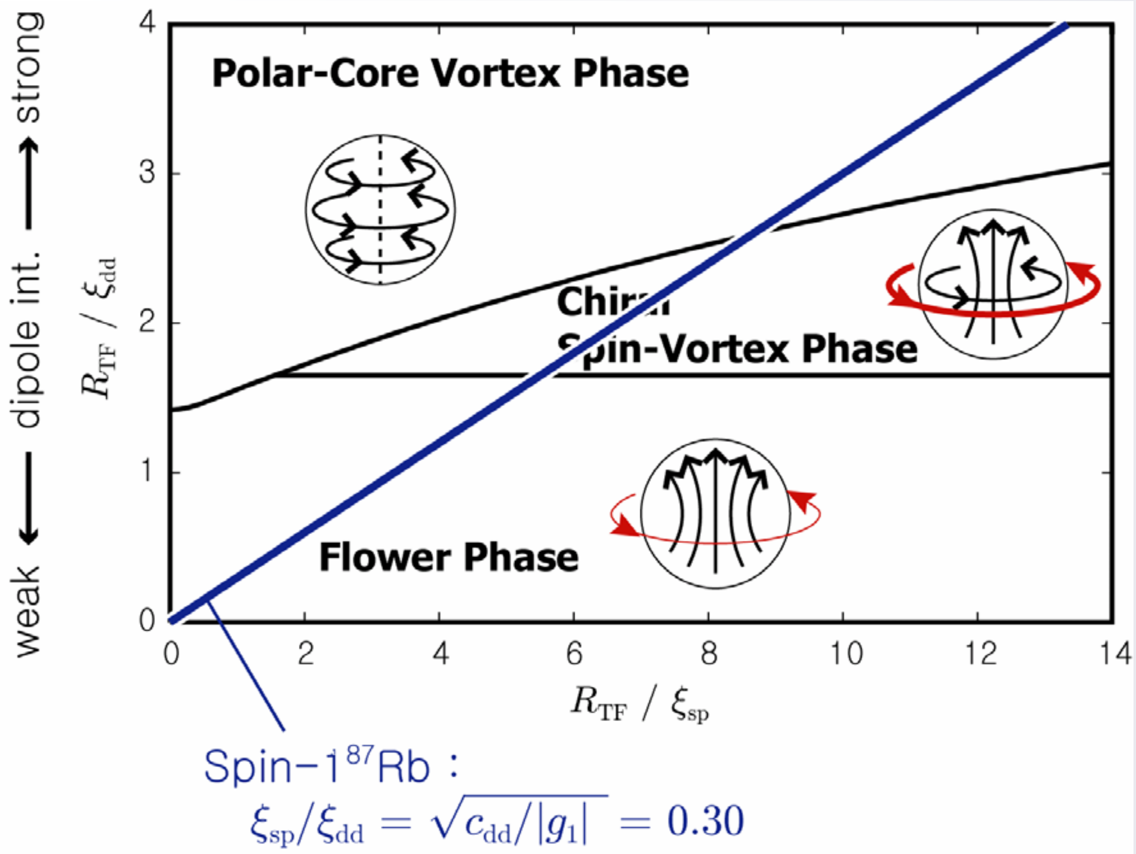

All three phases can be realized by changing the Thomas-Fermi radius, i.e., by changing the atomic number or the trap frequency.

Spin-1 ^{87}Rb BEC

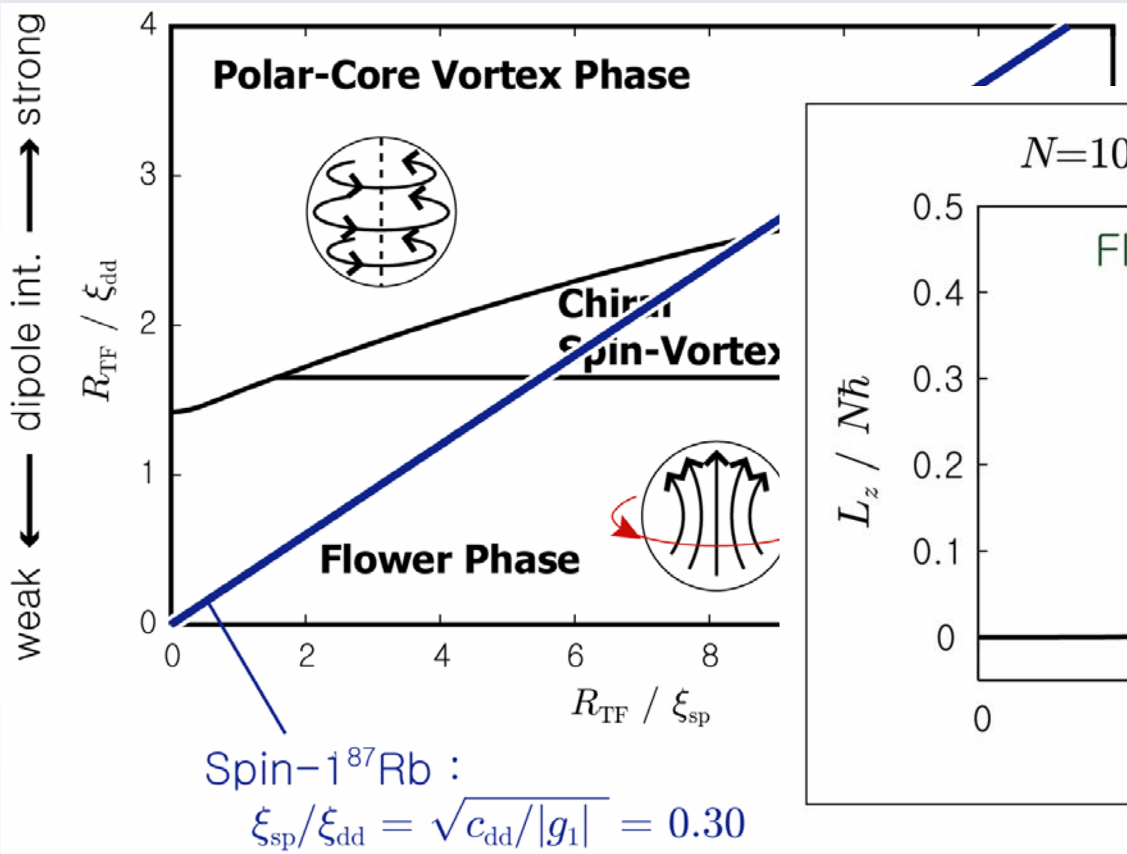

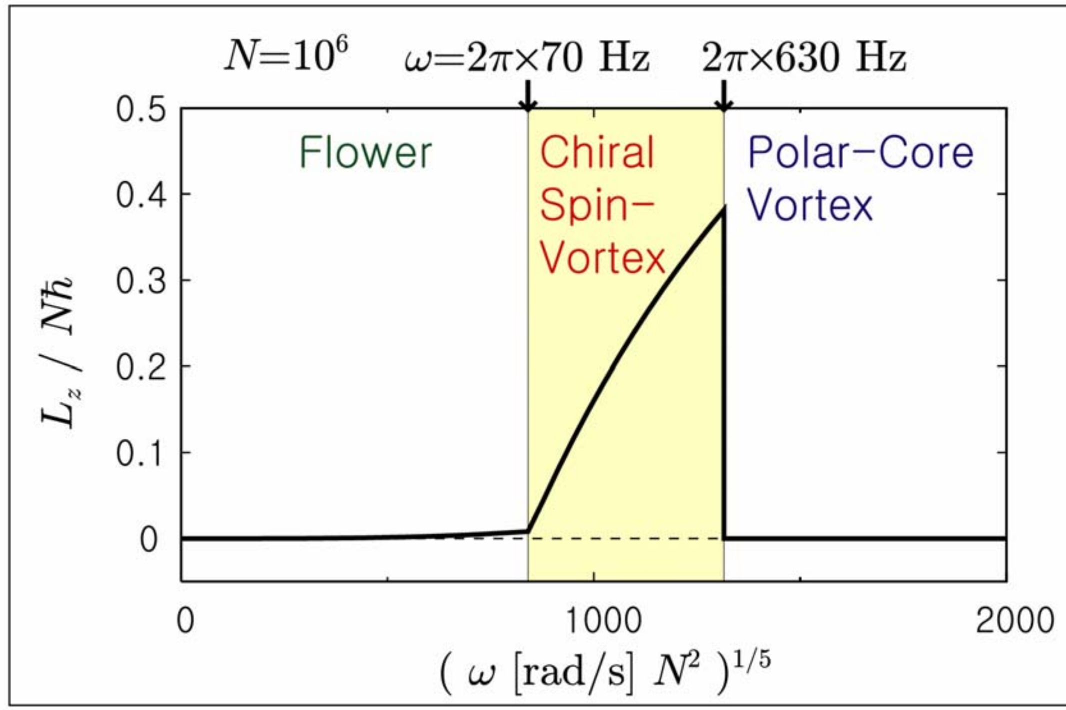

We find paticularly in the chiral spin-vortex state, that the orbital AM is increased by up to 40% of the full value of the quantized circulation.

Summary

Gaseous BEC --- mesoscopic system

Studying this system enables us to learn in detail when and how symmetry breaking occurs, and to identify the dynamics of symmetry breaking due to the long collision times.

Various types of symmetry breakings are experimentally accessible:

- **Soliton formation:** translation symmetry broken
- **Vortex nucleation:** axisymmetry broken
- **Spinor BEC:** rotational and chiral symmetries broken
  various spin textures spontaneously generated
  due to competition between conservation law,
  interaction, and geometry of the system
- **Dipolar BEC:** Einstein-de Haas effect
  ground-state circulation
  in the chiral spin-vortex phase